

A new uranyl niobate sheet in the cesium uranyl niobate $\text{Cs}_9[(\text{UO}_2)_8\text{O}_4(\text{NbO}_5)(\text{Nb}_2\text{O}_8)_2]$

S. Saad, S. Obbade*, S. Yagoubi¹, C. Renard, F. Abraham

UCCS-Equipe de Chimie du Solide, UMR CNRS 8181, USTL-ENSCL, B.P. 90108, 59652 Villeneuve d'Ascq Cedex, France

Received 25 October 2007; received in revised form 21 December 2007; accepted 2 January 2008

Available online 12 January 2008

Abstract

A new cesium uranyl niobate, $\text{Cs}_9[(\text{UO}_2)_8\text{O}_4(\text{NbO}_5)(\text{Nb}_2\text{O}_8)_2]$ or $\text{Cs}_9\text{U}_8\text{Nb}_5\text{O}_{41}$ has been synthesized by high-temperature solid-state reaction, using a mixture of U_3O_8 , Cs_2CO_3 and Nb_2O_5 . Single crystals were obtained by incongruent melting of a starting mixture with metallic ratio = $\text{Cs}/\text{U}/\text{Nb} = 1/1/1$. The crystal structure of the title compound was determined from single crystal X-ray diffraction data, and solved in the monoclinic system with the following crystallographic data: $a = 16.729(2) \text{ \AA}$, $b = 14.933(2) \text{ \AA}$, $c = 20.155(2) \text{ \AA}$, $\beta = 110.59(1)^\circ$, $P2_1/c$ space group and $Z = 4$. The crystal structure was refined to agreement factors $R_1 = 0.049$ and $wR_2 = 0.089$, calculated for 4660 unique observed reflections with $I \geq 2\sigma(I)$, collected on a BRUKER AXS diffractometer with $\text{MoK}\alpha$ radiation and a CCD detector.

In this structure the UO_7 uranyl pentagonal bipyramids are connected by sharing edges and corners to form a uranyl layer ${}_{\infty}^2[\text{U}_8\text{O}_{36}]$ corresponding to a new anion-sheet topology, and creating triangular, rectangular and square vacant sites. The two last sites are occupied by Nb_2O_8 entities and NbO_5 square pyramids, respectively, to form infinite uranyl niobate sheets ${}_{\infty}^2[(\text{UO}_2)_8\text{O}_4(\text{NbO}_5)(\text{Nb}_2\text{O}_8)_2]^{9-}$ stacking along the $[010]$ direction. The Nb_2O_8 entities result from two edge-shared NbO_5 square pyramids. The Cs^+ cations are localized between layers and ensured the cohesion of the structure.

The cesium cation mobility between the uranyl niobate sheets was studied by electrical measurements. The conductivity obeys the Arrhenius law in all the studied temperature domains. The observed low conductivity values with high activation energy may be explained by the strong connection of the Cs^+ cations to the infinite uranyl niobate layers and by the high density of these cations in the interlayer space without vacant site.

Infrared spectroscopy investigated at room temperature in the frequency range $400\text{--}4000 \text{ cm}^{-1}$, showed some characteristic bands of uranyl ion and niobium polyhedra.

© 2008 Elsevier Inc. All rights reserved.

Keywords: Solid-state synthesis; Single-crystal X-ray diffraction; Crystal structure; Uranyl niobate; Layered structure

1. Introduction

The chemistry of actinides has attracted a great deal of interest these last two decades with the assessment of nuclear waste disposal and improvement of reprocessing. In this connection, a large variety of new compounds resulting from the association of uranyl ion and various inorganic oxoanions (sulfate, phosphate, vanadate, tung-

state, molybdate, etc.) have been prepared and characterized. In this regard, a number of alkali metal uranyl oxoanion compounds have been recently reported and display a rich structural chemistry. The structural diversity is related to the variability of both the coordination chemistry of uranium (VI), which occurs as hexagonal, pentagonal and tetragonal bipyramids, and the oxoanion geometry, in particular with transition metal as central atom, which can be a tetrahedron, a square pyramid or an octahedron, and to the huge possibilities of linkage between these primary building units by corner or edge sharing. Our group has largely contributed to the identification of many new uranyl vanadates [1]. Among

*Corresponding author. Fax: +33 3 20 43 68 14.

E-mail address: said.obbade@ensc-lille.fr (S. Obbade).

¹Present address: Institute for Transuranium Element, Postfach 2340, 76125 Karlsruhe, Germany.

the alkali metals, cesium plays a particular role since cesium is an important fission product created during the irradiation of nuclear fuel. Niobium is both fission and activation product. Thus the knowledge of the cesium–uranium–niobium oxides is very important. We have recently initiated a program to prepare uranyl niobates and published two series of alkali metal uranyl niobates $AUNbO_6$ ($A = \text{Li, Na, K, Cs}$) [2] and $AU_2Nb_2O_{11.5}$ ($A = \text{Rb, Cs}$) [2]. The structure of $CsUNbO_6$ [3] is built from ${}^2_{\infty}[\text{UNbO}_6]^{2-}$ layers similar to the carnotite-type ${}^2_{\infty}[\text{UVO}_6]^{2-}$ layer common to numerous uranyl vanadates with the general formula $M_{2/n}{}^{n+}[(\text{UO}_2)_2\text{V}_2\text{O}_8] \cdot x\text{H}_2\text{O}$ ($n = 1, 2$) [1,4–13], such as $CsUVO_6$ [12] and the mineral carnotite $KUVO_6$ itself [13]. Owing to the linearity of the uranyl ion, and to the bond valence distribution in uranyl polyhedra, uranyl-containing bipyramids generally condense with uranyl ion parallel to one another and oxo atoms are almost exclusively terminal, thus two-dimensional layers are the most common structural arrangement in uranyl vanadates and uranyl compounds in general. However in $CsU_2Nb_2O_{11}$ parallel ${}^1_{\infty}[\text{UO}_5]^{4-}$ chains, of edge-shared UO_7 pentagonal bipyramids, and ${}^1_{\infty}[\text{Nb}_2\text{O}_8]^{6-}$ ribbons, of two edge-shared NbO_6 octahedra further linked by corners, are associated by edge sharing to form a three-dimensional open framework. The large tunnels parallel to the chains and ribbons are occupied by the Cs atoms [2].

Herein, we report the solid-state synthesis and the crystal structure determination of a new layered cesium uranyl niobate $Cs_9[(\text{UO}_2)_8\text{O}_4(\text{NbO}_5)(\text{Nb}_2\text{O}_8)_2]$. The infrared spectroscopy spectra and the electrical conductivity behaviors are compared to those of other previously reported cesium uranyl compounds.

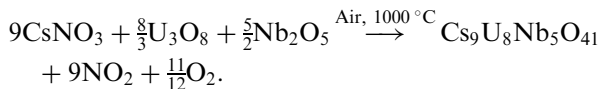
2. Experimental

2.1. Single crystal and powder synthesis

Single crystals of the cesium uranyl niobate $Cs_9[(\text{UO}_2)_8\text{O}_4(\text{NbO}_5)(\text{Nb}_2\text{O}_8)_2]$ were synthesized by solid-state reaction, using a mixture of U_3O_8 (Prolabo), Cs_2CO_3 (Aldrich) and Nb_2O_5 (Prolabo), with a metallic ratio $\text{Cs}/\text{U}/\text{Nb} = 1/1/1$. After grinding of the reagents in an agate mortar, the mixture was heated, using a tubular furnace, to 1400°C in a platinum crucible and maintained at this temperature for 2 days, and slowly cooled ($5^\circ\text{C}/\text{h}$) to room temperature. At the end of the thermal treatment, the molten mixture was washed with ethanol and yellowness crystals of $Cs_9[(\text{UO}_2)_8\text{O}_4(\text{NbO}_5)(\text{Nb}_2\text{O}_8)_2]$ were obtained, accompanied by single crystals of the recently studied compound $CsU_2Nb_2O_{11.5}$ [2] and non-identified powder. Energy dispersive spectroscopy (EDS) analysis of the yellow crystals using a JEOL-JSM 5300 scanning electron microscope (SEM) equipped with a PGT X-ray microanalysis system (IMIX) revealed the presence of the three starting metallic elements Cs, U, Nb in a ratio close to 9:8:5. The actual formula of the title compound, $Cs_9U_8Nb_5O_{41}$, has

been precisely established by crystal structure determination from single crystal X-ray diffraction data.

Pure powder sample of $Cs_9[(\text{UO}_2)_8\text{O}_4(\text{NbO}_5)(\text{Nb}_2\text{O}_8)_2]$ was prepared by solid-state reaction at 1000°C in air, according to the following reaction:



The homogeneous mixture was slowly heated in a platinum crucible to 1000°C and maintained at this temperature during 10 days. Several intermediate regrindings were realized in order to homogenize the mixture. To follow the reaction evolution and to check the sample purity, the resulting powder was examined by X-ray powder diffraction using a Guinier-De Wolff focusing camera and $\text{Cu}(K\alpha)$ radiation. The X-ray diffraction pattern of the obtained powder was similar to that of crushed single crystals and to that of calculated pattern from single crystal structure results. The density measured with an automated micromeritics occupies 1330 helium pycnometer using a 1-cm^3 cell, indicates a good agreement between the calculated and measured densities, with $Z = 4$ formula per unit cell ($\rho_{\text{mes}} = 5.94(2)$ and $\rho_{\text{cal}} = 5.95(3)\text{g}/\text{cm}^3$). Furthermore, the agreement of the measured and calculated densities confirms the purity of the prepared powder.

2.2. Electrical, thermal and spectroscopic measurements

For the electrical conductivity measurements, powder sample was pelletized at room temperature using a conventional cold press and then sintered at 1000°C during 25 h, followed by very slow cooling ($0.5^\circ\text{C}/\text{min}$), to room temperature. Gold electrodes were sputtered on both flat faces and measurements were done by AC impedance spectrometry in the frequency range $1\text{--}10^6\text{ Hz}$ using a Solartron 1170 frequency-response analyzer. Measurements were made at 20°C intervals over the range $200\text{--}800^\circ\text{C}$ on both heating and cooling. Before every measurement, the temperature was stabilized during 1 h.

To define the thermal stability domain, differential thermal analysis (DTA) was conducted in air using a SETARAM DTA 92-1600 apparatus thermal analyzer, between 20 and 1300°C with heating or cooling rate of $5^\circ\text{C}/\text{mn}$. The thermal measurements were carried out using a powder sample and a platinum crucible.

Infrared spectra were recorded using the KBr dispersion technique (1 mg of sample in 125 mg KBr) with a Bruker Vector 22 Fourier Transform Infrared Spectrometer, which covers the $400\text{--}4000\text{ cm}^{-1}$ range.

For unit cell parameters refinement, powder X-ray diffraction data have been collected with a Bruker D8 $\theta/2\theta$ diffractometer equipped by $\text{Cu}K\alpha$ radiation, using Bragg-Brentano geometry, in steps of 0.03° and a counting

time of 40 s per step, within an angular range of 10–90° in 2 θ . The unit cell parameters were refined from powder diffraction pattern using Rietveld method [14,15]. The refinement was carried out using the “*pattern matching*” option of Fullprof program [16], where only the profile parameters (cell dimensions, peak shapes, background, zero point correction and symmetry) have been refined. The peak shape was described by a pseudo-Voigt function with an asymmetry correction at low angles. In order to describe the angular dependence of the peak full-width at half-maximum (H), the formulation of Caglioti et al [17] was used: $H^2 = U \tan^2 \theta + V \tan \theta + W$ where U , V and W parameters were refined in the process.

2.3. Single crystal X-ray diffraction and crystallographic studies

A yellow crystal was selected under an optical microscope, mounted on a glass fiber and aligned on a Bruker three-circle X-ray diffractometer equipped with a SMART APEX charge coupled device (CCD) detector with a crystal-detector distance of 4.5 cm. Unit cell parameters and orientation matrix were determined using 900 reflections and refined on the whole of collected data. The intensity data were measured at room temperature using the MoK α radiation ($\lambda = 0.71073 \text{ \AA}$) selected by a graphite monochromator. For the crystal structure determination, single crystal X-ray diffraction intensities were collected by a combination of three sets of 600 frames. The individual frames were measured using a ω -scan technique with an omega rotation of 0.3° and an acquisition time of 40 s per frame. The Saintplus (V6.02) software [18] was used to extract reflection intensities from the collected 1800 frames and absorption corrections were applied with SADABS program [19], using a semi-empirical method. Monoclinic unit cell parameters were refined leading to $a = 16.729(2) \text{ \AA}$, $b = 14.9330(18) \text{ \AA}$, $c = 20.155(2) \text{ \AA}$ and $\beta = 110.59(1)^\circ$ from integrating 4801 individual reflections.

The intensity data collection, refinement information and crystallographic characteristics are given in Table 1. Systematic absences of reflections $0k0$, $k = 2n + 1$ and $h0l$, $l = 2n + 1$ were consistent with the $P2_1/c$ space group. The crystal structure was solved in this space group, using neutral atomic scattering factors from “International Tables for X-ray Crystallography” [20]. In a first step heavy atoms, U and Cs, were located by direct methods using SHELXS program [21], while the remaining atoms Nb and O were found from successive Fourier map analyses using the SHELXL option of the SHELXTL software [22]. The atomic positions for all atoms with anisotropic displacement parameters for cations and isotropic factors for oxygen atoms were included in the last cycles of refinement. The atomic positions, with isotropic and equivalent isotropic displacement parameters for oxygen and metallic atoms, respectively, are provided in Table 2.

Table 1

Crystal data, intensity collection and structure refinement parameters for Cs₉[(UO₂)₈O₄(NbO₅)(Nb₂O₈)₂]

Crystal data	
Crystal symmetry	Monoclinic
Space group	$P2_1/c$
Unit cell	$a = 16.729(2) \text{ \AA}$ $b = 14.933(2) \text{ \AA}$ $c = 20.155(2) \text{ \AA}$ $\beta = 110.59(1)^\circ$ $V = 4713.5(1) \text{ \AA}^3$
Z	4
Calculated density	$\rho_{\text{cal}} = 5.95(3) \text{ g/cm}^3$
Measured density	$\rho_{\text{mes}} = 5.94(2) \text{ g/cm}^3$
Data collection	
Temperature (K)	293(2)
Radiation Mo(K α)	0.71073 \AA
Scan mode	Omega
F(000)	7056
Recording angular range (deg)	3.62/29.32
Recording reciprocal space	$-22 \leq h \leq 22$ $-22 \leq k \leq 20$ $-26 \leq l \leq 27$
Number of reflections measured/independent	14,166/4801
Absorption μ (cm ⁻¹)	354.9
Color	Yellow
Size (mm)	0.088, 0.024, 0.116
Refinement	
Refined parameters/restraints	364/0
Goodness of fit on F^2	1.022
R_1 [$I > 2\sigma(I)$]	0.049
wR_2 [$I > 2\sigma(I)$]	0.088
R_1 for all data	0.061
wR_2 for all data	0.098
Largest diff peak and hole (e \AA^{-3})	2.887/−2.597

$$R_1 = \frac{\sum(|F_o| - |F_c|)}{\sum|F_o|}, \quad wR_2 = \frac{[\sum w(F_o^2 - F_c^2)^2 / \sum w(F_o^2)^2]^{1/2}}{[\sigma^2(F_o^2) + (0.02585P)^2]} \text{ with } P = (F_o^2 + 2F_c^2)/3.$$

Table 2

Atomic coordinates and isotropic equivalent displacement parameters (\AA^2) for Cs₉[(UO₂)₈O₄(NbO₅)(Nb₂O₈)₂]

Atom	Site	x	y	z	$U_{\text{iso}}/U_{\text{eq}}^*$
U1	4e	0.03301(8)	0.75766(10)	0.23566(6)	0.0137(3)*
U2	4e	0.80256(8)	0.75833(10)	0.14761(6)	0.0132(3)*
U3	4e	0.21434(8)	0.73372(10)	0.16218(6)	0.0125(3)*
U4	4e	0.61696(8)	0.71720(10)	0.21621(6)	0.0131(3)*
U5	4e	0.9769(8)	0.77269(10)	0.04031(6)	0.0135(3)*
U6	4e	0.85321(8)	0.73727(10)	0.34048(6)	0.0137(3)*
U7	4e	0.45535(8)	0.71598(10)	0.35604(6)	0.0130(3)*
U8	4e	0.37865(8)	0.76433(10)	0.51995(6)	0.0129(3)*
Nb1	4e	0.11289(19)	0.7280(2)	0.94889 (14)	0.0114(7)*
Nb2	4e	0.71830(19)	0.6916(2)	0.43118(14)	0.0116(7)*
Nb3	4e	0.61236(19)	0.7958(2)	0.51361(14)	0.0121(7)*
Nb4	4e	0.41160(19)	0.6508(2)	0.18476(15)	0.0118(7)*
Nb5	4e	0.22535(19)	0.8117(2)	0.86391(14)	0.0110(7)*
Cs1	4e	0.57212(16)	0.45741(18)	0.31087(12)	0.0289(6)*
Cs2	4e	0.71850(15)	0.97587(17)	0.24677(11)	0.0223(6)*
Cs3	4e	0.95064(15)	1.00835(18)	0.15157(12)	0.0328(7)*
Cs4	4e	0.52230(19)	0.49594(18)	0.09339(11)	0.0270(6)*
Cs5	4e	0.97436(15)	0.99149(18)	0.37023(13)	0.0310(6)*
Cs6	4e	0.62038(17)	0.96651(19)	0.04279(11)	0.0296(8)*

Table 2 (continued)

Atom	Site	<i>x</i>	<i>y</i>	<i>z</i>	$U_{\text{iso}}/U_{\text{eq}}^*$
Cs7	4e	0.84772(18)	0.47807(19)	0.43763(13)	0.0330(7)*
Cs8	4e	0.76679(16)	0.97010(20)	0.46525(13)	0.0393(8)*
Cs9	4e	0.77046(17)	0.45980(20)	0.18829(17)	0.0526(9)*
O1	4e	0.6404(16)	0.7610(14)	0.6077(9)	0.016(5)
O2	4e	0.2330(13)	0.7700(16)	0.9610(10)	0.016(5)
O3	4e	0.1312(13)	0.7686(16)	0.0435(10)	0.016(5)
O4	4e	0.8384(13)	0.7050(14)	0.4538(10)	0.010(5)
O5	4e	0.3576(13)	0.8760(15)	0.4926(10)	0.013(5)
O6	4e	0.5999(13)	0.7410(16)	0.4172(10)	0.016(5)
O7	4e	0.9649(14)	0.6546(15)	0.0388(11)	0.016(6)
O8	4e	0.1918(14)	0.7635(16)	0.7717(10)	0.019(6)
O9	4e	0.3407(12)	0.7771(15)	0.8962(19)	0.009(5)
O10	4e	0.7832(13)	0.8804(14)	0.1441(10)	0.008(5)
O11	4e	0.7314(11)	0.7524(13)	0.5227(8)	0.010(4)
O12	4e	0.7071(13)	0.7194(15)	0.3375(10)	0.014(5)
O13	4e	0.1033(12)	0.7815(14)	0.8561(9)	0.017(5)
O14	4e	0.9919(13)	0.7549(14)	0.9276(9)	0.010(5)
O15	4e	0.9866(14)	0.8917(16)	0.0361(11)	0.019(6)
O16	4e	0.6383(13)	0.5982(14)	0.2148(10)	0.008(5)
O17	4e	0.8675(14)	0.6208(16)	0.3295(11)	0.020(6)
O18	4e	0.7494(12)	0.7556(14)	0.2332(9)	0.016(5)
O19	4e	0.0841(14)	0.7728(16)	0.1478(10)	0.018(5)
O20	4e	0.3492(14)	0.6808(15)	0.2476(10)	0.015(5)
O21	4e	0.9247(13)	0.7866(15)	0.1247(10)	0.015(5)
O22	4e	0.4919(13)	0.7700(15)	0.4789(10)	0.013(5)
O23	4e	0.9142(14)	0.7667(17)	0.2593(11)	0.023(6)
O24	4e	0.3207(13)	0.7060(14)	0.1094(10)	0.019(5)
O25	4e	0.8112(14)	0.6367(15)	0.1456(11)	0.016(6)
O26	4e	0.0536(14)	0.8743(15)	0.2585(10)	0.016(6)
O27	4e	0.1867(13)	0.6162(15)	0.1479(10)	0.014(5)
O28	4e	0.4415(13)	0.8285(15)	0.3275(10)	0.014(5)
O29	4e	0.4061(14)	0.5320(16)	0.1759(11)	0.019(6)
O30	4e	0.0211(13)	0.6386(14)	0.2223(10)	0.011(5)
O31	4e	0.8398(15)	0.8543(16)	0.3580(11)	0.022(6)
O32	4e	0.4674(13)	0.6037(14)	0.3829(10)	0.008(5)
O33	4e	0.3993(15)	0.6508(16)	0.5453(11)	0.020(6)
O34	4e	0.6233(15)	0.9119(16)	0.5128(11)	0.022(6)
O35	4e	0.5100(14)	0.6839(15)	0.2659(11)	0.016(5)
O36	4e	0.2493(15)	0.8476(17)	0.1794(12)	0.027(6)
O37	4e	0.1265(16)	0.6162(17)	0.9478(12)	0.027(6)
O38	4e	0.4804(13)	0.6858(14)	0.128(1)	0.019(5)
O39	4e	0.5889(15)	0.8334(17)	0.2143(11)	0.025(6)
O40	4e	0.7003(15)	0.5777(16)	0.4387(11)	0.023(6)
O41	4e	0.2264(15)	0.9287(16)	0.8612(11)	0.023(6)

Note: U_{eq} is defined as one third of the trace of the orthogonalized U_{ij} tensor. The U_{eq} values are defined by $U_{\text{eq}} = 1/3(\sum_i \sum_j U_{ij} a_i^* a_j)$.

3. Results and discussion

3.1. Crystal structure description

The principal interatomic distances and bond valence sums calculated using Burns parameters for uranium atoms [23] and Brese and O'Keeffe data for the other atoms [24] are presented in Table 3.

The structure of $\text{Cs}_9[(\text{UO}_2)_8\text{O}_4(\text{NbO}_5)(\text{Nb}_2\text{O}_8)_2]$, consists of bidimensional anionic uranyl niobate layers ${}^2_{\infty}[(\text{UO}_2)_8\text{O}_4(\text{NbO}_5)(\text{Nb}_2\text{O}_8)_2]^{9-}$, separated and charge-balanced by Cs^+ cations. The infinite uranyl niobate layer is constructed from two types of polyhedral entities, UO_7 pentagonal bipyramids and NbO_5 square pyramids. The

$\text{U}(1)\text{O}_7$ – $\text{U}(6)\text{O}_7$ polyhedra are associated by sharing edges to form a hexameric cluster $[(\text{U}_6\text{O}_{30})]$ which can be pictured by the capital I letter and can be considered as a secondary building unit (SBU) (Fig. 1a). This entity was observed for the first time in alkaline uranyl tungstates $M_2(\text{UO}_2)_2(\text{WO}_5)\text{O}$ ($M = \text{K}, \text{Rb}, \text{Cs}$) [25–27] and in the molybdate $\text{Ti}_2(\text{UO}_2)_2(\text{MoO}_5)\text{O}$ [28], where the cluster is completed by sharing edges with two other UO_7 polyhedra to form a $[\text{U}_8\text{O}_{40}]$ unit. The two last $\text{U}(7)\text{O}_7$ and $\text{U}(8)\text{O}_7$ pentagonal bipyramids are associated by sharing the $\text{O}(2)$ – $\text{O}(22)$ edge to form a $[\text{U}_2\text{O}_{12}]$ dimeric unit (Fig. 1b).

The hexameric SBU are associated by sharing two opposite edges with two other SBU to form infinite ${}^1_{\infty}[\text{UO}_6\text{O}_{28}]$ uranyl ribbons parallel to the [001] direction, Fig. 2b. Two parallel infinite ribbons are linked together by $[\text{U}_2\text{O}_{12}]$ units to form infinite ${}^2_{\infty}[\text{U}_8\text{O}_{36}]$ uranyl layers parallel to the (010) plane (Fig. 2b). The corresponding arrangement creates two types of holes. The square holes are occupied by $\text{Nb}(4)$ atoms whose coordination is completed by a fifth oxygen atom to form a square pyramid (Fig. 3a) which is linked by sharing two edges of the basal square with two $[\text{U}_2\text{O}_{12}]$ dimers and the other two edges with two adjacent infinite uranyl ribbons ${}^1_{\infty}[\text{U}_6\text{O}_{28}]$. The second holes which can be pictured by the capital T letter are formed from two squares and three triangles, the square sites are edge-shared to form a rectangular hole occupied by a Nb_2O_8 dimeric unit of two edge-shared NbO_5 square pyramids (Fig. 3b) connected to the uranium polyhedra sheet by sharing edges with two successive $[\text{U}_6\text{O}_{30}]$ clusters of the same infinite ribbons and with one $[\text{U}_2\text{O}_{12}]$ dimer. Recently Burns [29] has reviewed the crystal structures of 368 inorganic compounds containing U^{6+} , among them 204 contain sheets and are classified according to their sheet anion-topology. The sheet in $\text{Cs}_9[(\text{UO}_2)_8\text{O}_4(\text{NbO}_5)(\text{Nb}_2\text{O}_8)_2]$ corresponds to a new anion-topology containing pentagons, squares and triangles (Fig. 2a), all the pentagons and squares are occupied by uranium and niobium atoms, respectively, whereas the triangles remain vacant (Fig. 2c). One Nb_2O_8 dimer can be referenced as *ud* with a tetragonal pyramid that point *up* and one *down*. In the layers the dimers have the same orientation along [100], *ud/ud*, but alternate along [001] to form the succession *ud/du*. Similarly the isolated NbO_5 pyramids have the same orientation along [100], *u/u* or *d/d*, but alternate along [001], *u/d*, in such a way that one NbO_5 pyramid *up* is surrounded by two *ud* and two *du* dimers with the four closest pyramids of the dimers *up*.

There are eight crystallographically unique uranium atoms in $\text{Cs}_9[(\text{UO}_2)_8\text{O}_4(\text{NbO}_5)(\text{Nb}_2\text{O}_8)_2]$. All the $\text{U}(\text{VI})$ atoms are bonded to two oxygen atoms at short distances in the range 1.75(2)–1.85(2) Å, forming nearly linear $(\text{O}=\text{U}=\text{O})^{2+}$ uranyl ions with an $\text{O}-\text{U}-\text{O}$ angle ranging from 174(1) to 179(1)° and an average $\langle \text{U}=\text{O} \rangle$ bond length of 1.79(2) Å, in perfect agreement with the average value of 1.79(4) Å calculated from 98 UO_7 polyhedra [23]. However the $\text{U}=\text{O}$ distances are shorter in the UO_7

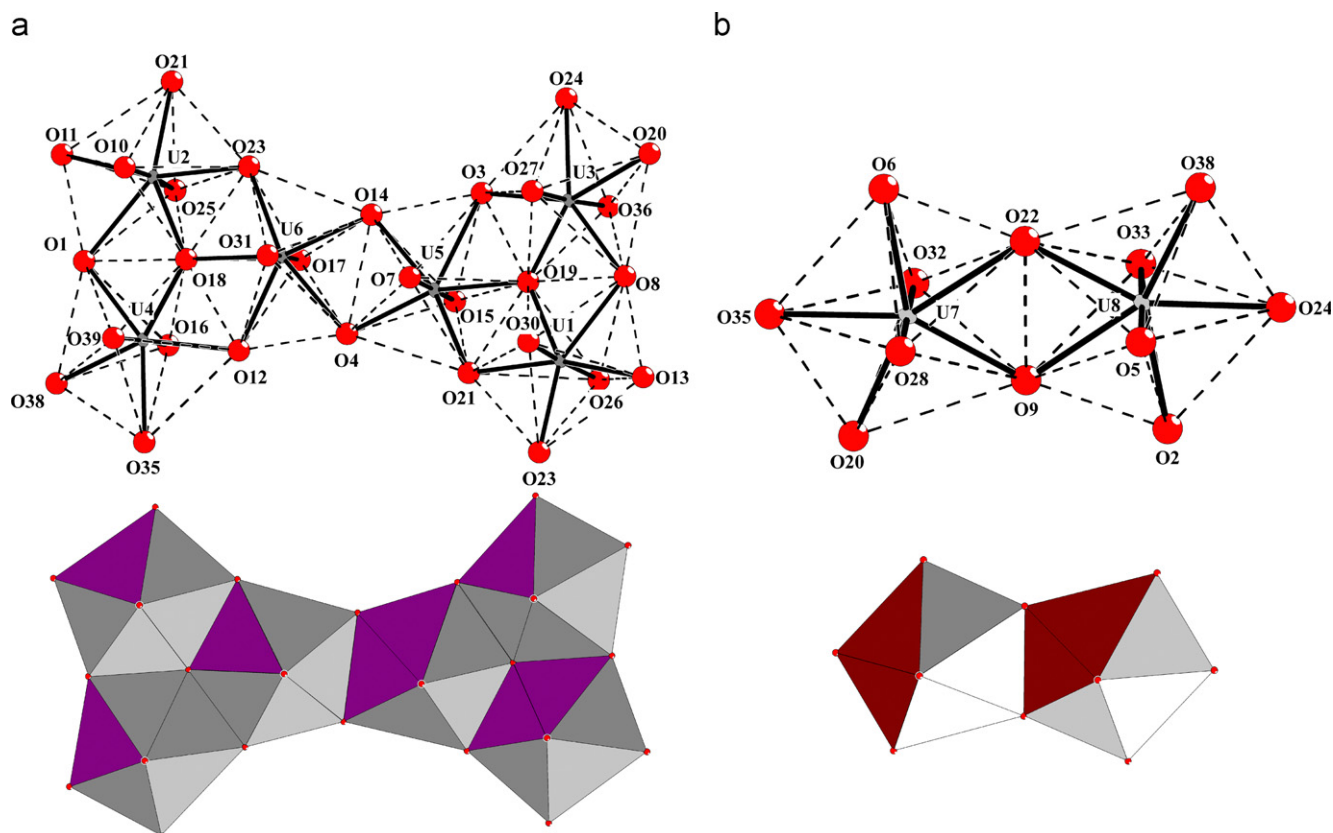
Table 3

Bond distances (Å), uranyl angles (deg) and bond valences S_{ij} in $\text{Cs}_9[(\text{UO}_2)_8\text{O}_4(\text{NbO}_5)(\text{Nb}_2\text{O}_8)_2]$

Atoms	Distance	S_{ij}	Atoms	Distance	S_{ij}	Atoms	Distance	S_{ij}
U1–O30	1.80(2)	1.622	U2–O25	1.82(2)	1.561	U3–O36	1.79(2)	1.653
U1–O26	1.80(2)	1.622	U2–O10	1.85(2)	1.473	U3–O27	1.81(2)	1.591
U1–O23	2.21(2)	0.736	U2–O18	2.20(22)	0.748	U3–O19	2.17(2)	0.795
U1–O19	2.23(2)	0.708	U2–O21	2.29(2)	0.631	U3–O3	2.36(2)	0.547
U1–O13	2.37(2)	0.543	U2–O23	2.37(2)	0.541	U3–O8	2.37(2)	0.541
U1–O21	2.37(2)	0.541	U2–O11	2.38(1)	0.529	U3–O24	2.41(2)	0.501
U1–O8i	2.51(2)	0.413	U2–O1	2.56(2)	0.375	U3–O20	2.44(2)	0.473
$\sum S_{ij}$		6.185			5.858			6.101
$O30-U1-O26 = 174(1)$			$O25-U2-O10 = 175(1)$			$O36-U3-O27 = 176(1)$		
U4–O39	1.79(3)	1.653	U5–O7	1.77(2)	1.718	U6–O17	1.78(2)	1.686
U4–O16	1.81(2)	1.591	U5–O15	1.79(2)	1.653	U6–O31	1.81(2)	1.591
U4–O18	2.20(2)	0.756	U5–O21	2.18(2)	0.78	U6–O23	2.25(3)	0.682
U4–O1	2.38(2)	0.535	U5–O19	2.27(2)	0.643	U6–O18	2.26(2)	0.663
U4–O12	2.38(2)	0.532	U5–O4	2.38(2)	0.531	U6–O14	2.37(2)	0.541
U4–O35	2.39(3)	0.52	U5–O14	2.39(2)	0.524	U6–O4	2.43(2)	0.481
U4–O38	2.40(2)	0.51	U5–O3	2.56(2)	0.375	U6–O12	2.44(2)	0.473
$\sum S_{ij}$		6.097			6.224			6.117
$O5-U4-O33 = 176(1)$			$O7-U5-O15 = 177(1)$			$O17-U6-O31 = 176(1)$		
U7–O32	1.75(2)	1.786	U8–O5	1.75(2)	1.786			
U7–O28	1.76(2)	1.752	U8–O33	1.77(2)	1.718			
U7–O6	2.33(2)	0.584	U8–O22	2.32(2)	0.596			
U7–O9	2.33(22)	0.582	U8–O2	2.36(2)	0.551			
U7–O20	2.34(2)	0.573	U8–O38	2.36(2)	0.546			
U7–O35	2.35(3)	0.562	U8–O24	2.37(2)	0.541			
U7–O22	2.47(2)	0.449	U8–O9	2.43(2)	0.541			
$\sum S_{ij}$		6.288			6.222			
$O32-U7-O22 = 179(1)$			$O39-U8-O16 = 179(1)$					
Nb1–O37	1.69(3)	1.817	Nb2–O40	1.74(2)	1.588	Nb3–O34	1.74(2)	1.545
Nb1–O3	1.92(2)	0.976	Nb2–O12	1.88(2)	1.093	Nb3–O1	1.86(2)	1.145
Nb1–O14	1.96(2)	0.876	Nb2–O4	1.91(2)	1.003	Nb3–O22	1.92(2)	0.95
Nb1–O13	1.99(2)	0.812	Nb2–O11	2.00(2)	0.790	Nb3–O11	2.04(2)	0.704
Nb1–O2	2.04(2)	0.706	Nb2–O6	2.04(2)	0.706	Nb3–O6	2.05(2)	0.687
$\sum S_{ij}$		5.187			5.180			5.031
Nb4–O29	1.78(2)	1.425	Nb5–O41	1.75(2)	1.545			
Nb4–O24	1.92(2)	0.976	Nb5–O9	1.88(2)	1.087			
Nb4–O35	1.93(2)	0.95	Nb5–O8	1.88(2)	1.058			
Nb4–O38	1.96(2)	0.876	Nb5–O2	2.01(2)	0.745			
Nb4–O20	1.96(3)	0.876	Nb5–O13	2.04(2)	0.706			
$\sum S_{ij}$		5.103			5.141			
Cs1–O39	3.16(2)	0.134	Cs2–O39	2.94(2)	0.243	Cs3–O26	3.00(2)	0.207
Cs1–O33	3.21(2)	0.117	Cs2–O41	3.00(2)	0.207	Cs3–O41	3.03(2)	0.191
Cs1–O40	3.25(2)	0.105	Cs2–O27	3.01(2)	0.201	Cs3–O30	3.10(2)	0.158
Cs1–O16	3.30(2)	0.092	Cs2–O10	3.01(2)	0.201	Cs3–O15	3.13(2)	0.146
Cs1–O29	3.32(2)	0.087	Cs2–O31	3.04(2)	0.186	Cs3–O13	3.25(2)	0.105
Cs1–O28	3.33(2)	0.085	Cs2–O29	3.12(2)	0.151	Cs3–O10	3.35(2)	0.080
Cs1–O36	3.35(2)	0.080	Cs2–O20	3.28(2)	0.097	Cs3–O21	3.36(2)	0.078
Cs1–O32	3.43(2)	0.065	Cs2–O18	3.36(2)	0.078	Cs3–O17	3.38(2)	0.074
Cs1–O35	3.56(2)	0.046	Cs2–O32	3.80(2)	0.024	Cs3–O35	3.92(2)	0.017
$\sum S_{ij}$		0.811			1.387			1.056
Cs4–O34	2.90(2)	0.271	Cs5–O30	2.90(2)	0.271	Cs6–O40	2.93(2)	0.250
Cs4–O28	2.91(2)	0.264	Cs5–O37	2.95(2)	0.237	Cs6–O41	3.04(2)	0.186
Cs4–O16	2.96(2)	0.230	Cs5–O31	2.99(2)	0.213	Cs6–O10	3.05(2)	0.181
Cs4–O29	3.02(2)	0.196	Cs5–O7	3.00(2)	0.207	Cs6–O32	3.19(2)	0.124
Cs4–O34	3.05(2)	0.181	Cs5–O27	3.19(2)	0.124	Cs6–O33	3.23(2)	0.111
Cs4–O38	3.06(2)	0.176	Cs5–O26	3.46(2)	0.060	Cs6–O32	3.50(2)	0.054
Cs4–O5	3.38(2)	0.074	Cs5–O14	3.84(2)	0.021	Cs6–O1	3.61(2)	0.040
Cs4–O5	3.56(2)	0.046	Cs5–O23	3.96(2)	0.015	Cs6–O11	3.85(2)	0.020
Cs4–O22	3.65(2)	0.036				Cs6–O6	3.94(2)	0.016
$\sum S_{ij}$		1.474			1.148			0.982

Table 3 (continued)

Atoms	Distance	S_{ij}	Atoms	Distance	S_{ij}	Atoms	Distance	S_{ij}
Cs7–O40	2.89(2)	0.278	Cs8–O37	2.97(2)	0.224	Cs9–O25	2.93(2)	0.250
Cs7–O15	2.93(2)	0.250	Cs8–O34	3.01(2)	0.201	Cs9–O26	3.04(2)	0.186
Cs7–O36	3.05(2)	0.181	Cs8–O31	3.32(2)	0.087	Cs9–O16	3.21(2)	0.117
Cs7–O15	3.14(2)	0.142	Cs8–O29	3.39(2)	0.072	Cs9–O36	3.26(2)	0.102
Cs7–O17	3.15(2)	0.138	Cs8–O5	3.40(2)	0.070	Cs9–O8	3.44(2)	0.036
Cs7–O3	3.16(2)	0.134	Cs8–O27	3.44(2)	0.036	Cs9–O17	3.64(2)	0.037
Cs7–O4	3.41(2)	0.068	Cs8–O11	3.571(19)	0.044	Cs9–O5	3.74(2)	0.028
Cs7–O19	3.87(2)	0.020	Cs8–O7	3.63(2)	0.038	Cs9–O37	3.89(2)	0.019
			Cs8–O25	3.80(2)	0.024	Cs9–O28	3.96(2)	0.015
ΣS_{ij}		1.211			0.823			0.817

Fig. 1. The oxygen polyhedra around uranium atoms and the labeling scheme in (a) the $[U_6O_{30}]$ hexameric building unit and (b) the $[U_2O_{12}]$ dimeric unit.

polyhedra pertaining to the $[U_2O_{12}]$ dimeric units than in the UO_7 polyhedra of the $[U_6O_{30}]$ clusters. Each uranyl ion environment is completed in its equatorial plane by five other oxygen atoms at longer distances ranging from 2.17(2) to 2.56(2) Å, to form a UO_7 pentagonal bipyramid. The average $\langle U-O \rangle$ bond length for equatorial oxygen atoms of 2.35(2) Å is also in agreement with the average value of 2.37(9) Å calculated by Burns et al. [23]. However the U–O distances are more dispersed in the UO_7 polyhedra of the $[U_6O_{30}]$ clusters with the shortest distances corresponding to oxygen atoms shared between three UO_7 polyhedra. These bond distances can be used to calculate bond valence sums for the U(1)–U(8) atoms from

5.86 to 6.29 valence units (vu) that are consistent with hexavalent uranium.

There are five crystallographically unique niobium atoms all bonded to five oxygen atoms forming square pyramids with apical Nb–O bonds (1.69(3)–1.78(2) Å) shorter than the Nb–O bonds with oxygen atoms of the square bases (1.86(2)–2.05(2) Å) that are all shared with UO_7 polyhedra, whereas the Nb–O axial bonds are parallel to the $U=O$ bonds and the corresponding oxygen atoms not shared between polyhedra of the highest valence metal atoms (U and Nb). The longest Nb–O distances involve the oxygen atoms O(2), O(13) and O(6), O(11) bridging the two pairs of NbO_5 polyhedra to form the $[Nb(1)Nb(5)O_8]$ and

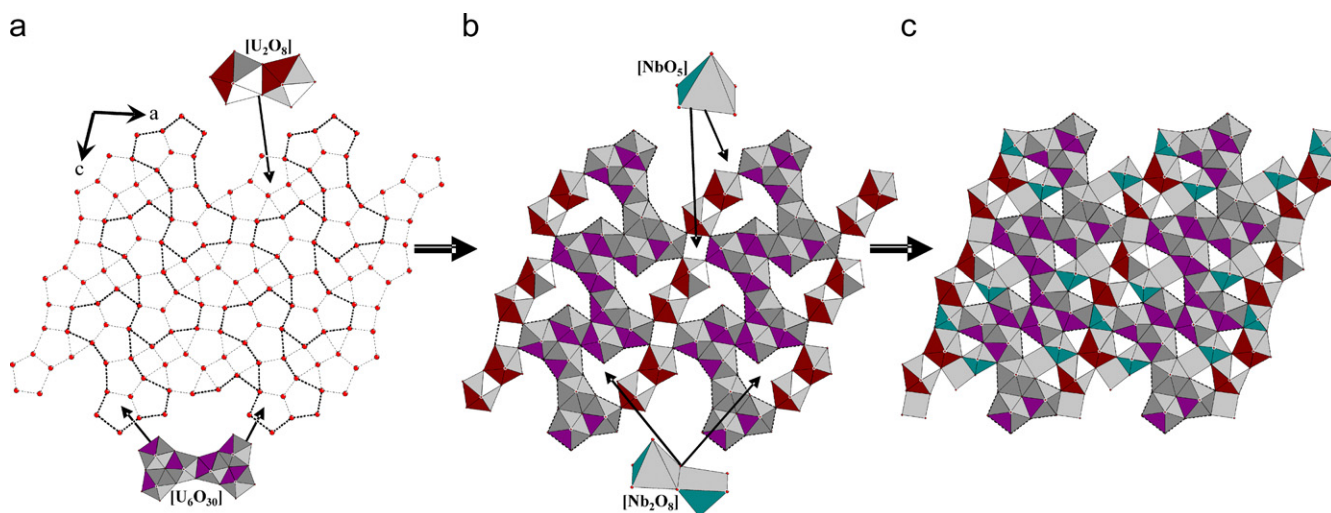


Fig. 2. The new anion sheet-topology in $\text{Cs}_9[(\text{UO}_2)_8\text{O}_4(\text{NbO}_5)(\text{Nb}_2\text{O}_8)_2]$ (a), with the pentagons occupied by uranium atoms to create an uranium layer ${}^2_{\infty}[\text{U}_8\text{O}_{36}]$ (b), leading to square holes occupied by NbO_5 and Nb_2O_8 units to form the two-dimensional uranyl niobate layer ${}^2_{\infty}[(\text{UO}_2)_8\text{O}_4(\text{NbO}_5)(\text{Nb}_2\text{O}_8)_2]^{9-}$ (c).

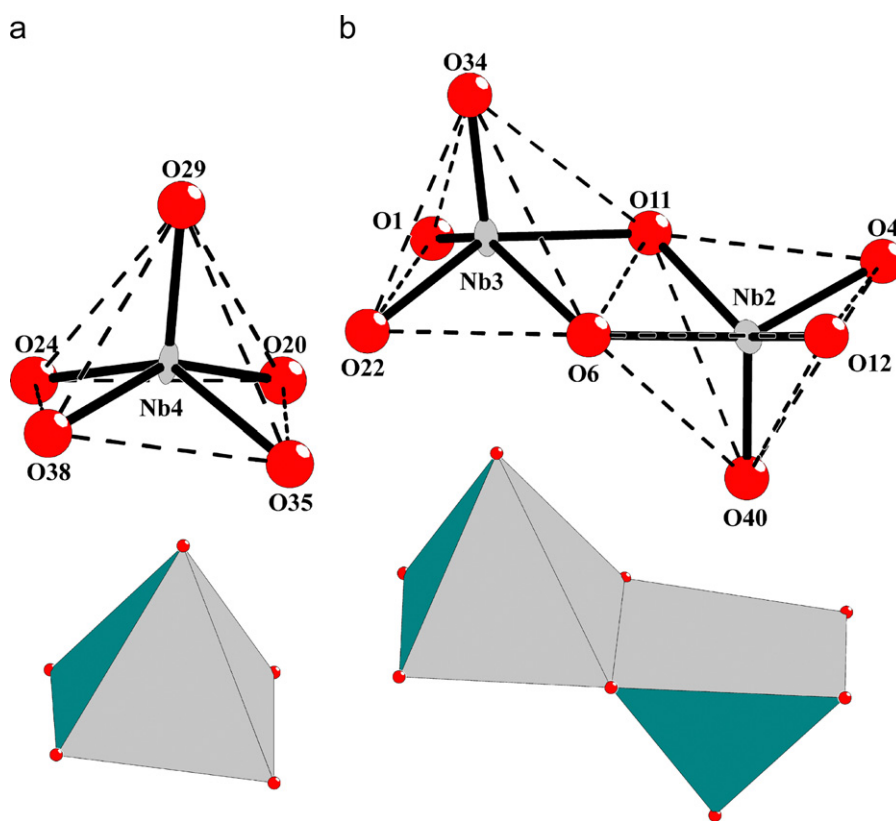


Fig. 3. The niobium atoms coordination and the labeling scheme in (a) the NbO_5 square pyramid and (b) the Nb_2O_8 dimeric entities of two edge-shared NbO_5 square pyramids.

$[\text{Nb}(2)\text{Nb}(3)\text{O}_8]$ dimeric units (Fig. 3b). The valence bond sums in the range 5.03–5.19 vu are in agreement with the +5 formal charge of niobium atoms.

Niobium atoms in square pyramidal coordination were already observed in numerous uranyl niobates as, for example, in the layered alkaline uranyl niobate family MUNbO_6 ($M = \text{Li}, \text{K}, \text{Rb}, \text{Cs}$) [2,3,30]. For $M = \text{Li}, \text{K},$

Rb , the NbO_5 pyramids are corner shared to form ${}^1_{\infty}[\text{NbO}_4]$ chains associated with parallel ${}^1_{\infty}[\text{UO}_5]$ chains of edge-shared UO_7 polyhedra to build a ${}^2_{\infty}[\text{UNbO}_6]^{2-}$ layer with uranophane sheet anion-topology. For $M = \text{K}$ and Rb , the orientation of the NbO_5 pyramids leads to corrugated layers separated by alkaline metals. For $M = \text{Li}$, the connection of two layers through a cation–cation

interaction $U=O\cdots Nb-O$ introduce a sixth oxygen atom at long distance (2.425(12) Å) in the Nb coordination to create a strongly distorted NbO_6 octahedron. $CsUNbO_6$ adopts a structure derived from the mineral carnotite and contains $[Nb_2O_8]$ dimers of edge-shared NbO_5 square pyramids associated with $[U_2O_{12}]$ entities of edge-shared UO_7 polyhedra to form a ${}^2_{\infty}[(UO_2)_2V_2O_8]^{2-}$ layer with the francevillite sheet anion-topology [29]. Analogous $[V_2O_8]$ dimers have been observed in the large family of compounds $M_{2/p}^{p+}(UO_2)_2V_2O_8 \cdot xH_2O$ (M = mono or divalent cations) derived from the carnotite mineral [1,4–13].

The nine crystallographically independent cesium atoms occupy the interspaces between the uranyl niobate layers stacked along the [010] direction (Fig. 4) and insure the cohesion of the structure, the shortest Cs–O distances correspond to bonds with oxygen atoms that belong to uranyl ions or are apical oxygen atoms of NbO_5 square

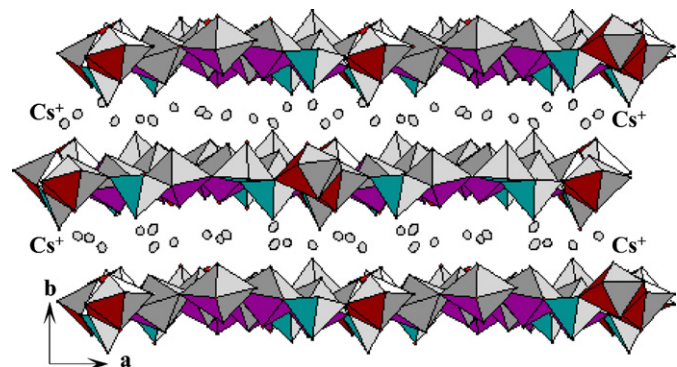


Fig. 4. The staking along the [010] direction of the ${}^2_{\infty}[(UO_2)_8O_4(NbO_5)(Nb_2O_8)_2]^{p-}$ layers in $Cs_9[(UO_2)_8O_4(NbO_5)(Nb_2O_8)_2]$ with Cs^+ cations in the interlayer space.

pyramids. Considering Cs–O distances lower than 3.80 Å, the coordination number for the cesium atoms varies from 6 to 9, the oxygen atoms forming distorted polyhedra with average Cs–O distances varying from 3.10 to 3.34 Å and bond valence sums spread over a broad domain from 0.78 to 1.47 vu. The Cs atoms form approximately a close-packed array parallel to the (010) plane.

Three types of oxygen atoms exist in this compound. (i) The terminal oxygen of the uranyl ions and the apical oxygen of the NbO_5 square pyramids are strongly bonded to the uranium or niobium atoms and their valence practically satisfied by the U–O or the Nb–O bond, the S_{ij} for these bonds varying from 1.47 to 1.78 vu for the eight independent uranyl ions and from 1.43 to 1.82 vu for the five independent niobate polyhedra, thus the coordination of these oxygen atoms are only completed by Cs^+ ions. (ii) The oxygen atoms of the basal square of the NbO_5 square pyramids, which are shared with another NbO_5 entity or with UO_7 pentagonal bipyramids. (iii) The oxygen atoms O(18), O(19), O(21) and O(23) which pertain only to the equatorial base of UO_7 bipyramids are shared between three UO_7 polyhedra. For the three types, the valence bond sums calculated for oxygen atoms, ranging from 1.83 and 2.33 vu with an average value of 2.06 vu, are in agreement with their ion oxide form.

3.2. Powder X-ray diffraction and cell parameters refinement

The unit cell parameters are refined from powder data to $a = 16.722(1)$, $b = 14.921(1)$, $c = 20.120(1)$ Å, $\beta = 110.60(1)^\circ$ and profile reliability factors $R_p = 0.058$ and $R_{wp} = 0.080$. The good agreement between observed and calculated powder X-ray diffraction diagrams are shown in Fig. 5.

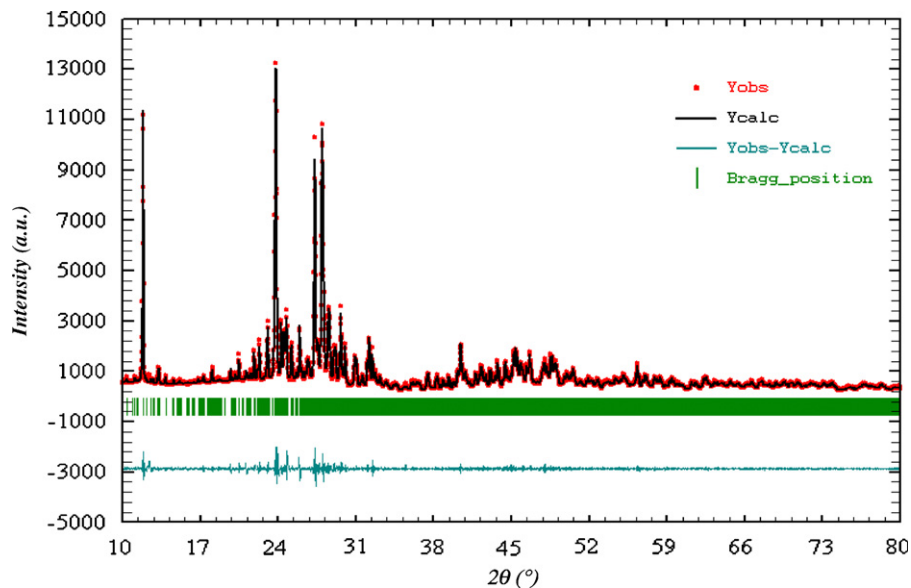


Fig. 5. Observed (Y_{obs}), calculated (Y_{cal}) and difference profiles ($Y_{obs}-Y_{cal}$) from Rietveld refinement of powder X-ray diffraction data of $Cs_9[(UO_2)_8O_4(NbO_5)(Nb_2O_8)_2]$. Allowed reflections are indicated by vertical lines.

3.3. Electrical and thermal properties

The bidimensional structures of the alkaline uranyl-bearing compounds with alkaline cations located between layers are generally favorable to the mobility of these cations and give significant cationic electrical conductivities. Thus, ionic conductivity measurements for $\text{Cs}_9[(\text{UO}_2)_8\text{O}_4(\text{NbO}_5)(\text{Nb}_2\text{O}_8)_2]$ were performed and compared with these of other recently reported CsUNbO_6 and $\text{CsU}_2\text{Nb}_2\text{O}_{11.5}$ compounds, exhibiting layered and tunneled structures, respectively, Fig. 6. For all compounds, electrical conductivity behavior obeys, in the studied temperature domain, to the Arrhenius law, with a linear evolution of $\log \sigma$ according to $1/T$ and an activation energy value of 0.79 eV for $\text{Cs}_9[(\text{UO}_2)_8\text{O}_4(\text{NbO}_5)(\text{Nb}_2\text{O}_8)_2]$. It can be seen that the cationic mobility in these materials is very sensitive to their structural types, comparing to the tunneled compound $\text{CsU}_2\text{Nb}_2\text{O}_{11.5}$ where the Cs^+ cations are located at the center of large mono-dimensional tunnels [2]. The low conductivity and high activation energy observed in the compound under study may be explained by the strong connection of the Cs^+ cations to the infinite layers $[(\text{UO}_2)_8\text{O}_4(\text{NbO}_5)(\text{Nb}_2\text{O}_8)_2]^{9-}$ and the cationic density between the layers. The conductivity of CsUNbO_6 is lower to that of the studied compounds, with larger activation energy, while the interlayer distances are comparable, the cationic density is lower and the coordination number higher.

The DTA experiment carried out from 25 to 1300 °C, did not evidence any phase transition. The X-ray powder diffraction analysis of the residue after DTA measurement showing that the phase is stable until 1300 °C. The melting temperature was estimated by heating the sample in a furnace at 50 °C intervals. The compound melts between

1350 and 1400 °C, slow cooling of the fused compound to 1000 °C and quenching from this temperature give a mixture of single crystals of CsUNbO_6 [3] and $\text{CsU}_2\text{Nb}_2\text{O}_{11.5}$ [2] accompanied by black powder of U_3O_8 . Refinement of the structure from an as-prepared crystal of CsUNbO_6 confirms the results of Gasperin et al. [3].

3.4. Infrared spectroscopy

Infrared spectroscopy measurements have been carried out in the spectral domain from 400 to 1000 cm^{-1} , for $\text{Cs}_9[(\text{UO}_2)_8\text{O}_4(\text{NbO}_5)(\text{Nb}_2\text{O}_8)_2]$ and for the layered compound CsUNbO_6 which can be written $\text{Cs}_2[(\text{UO}_2)_2(\text{Nb}_2\text{O}_8)]$. The comparison of both spectra given in Fig. 7 reveals a close similarity between them. In order to interpret the different vibration bands observed in the infrared spectra, three different groups can be considered in the layers: UO_7 pentagonal bipyramids, NbO_5 square pyramids and Nb_2O_8 dimeric units. The uranium atoms in pentagonal bipyramid coordination is characterized by two different vibration domains, corresponding to $[\text{O}=\text{U}=\text{O}]$ uranyl ion and $\text{U}-\text{O}_{\text{eq}}$ equatorial vibrations. The bands observed in the range 400–618 cm^{-1} may be assigned to the $\text{U}-\text{O}_{\text{eq}}$ vibrations between uranium and equatorial oxygen atoms. The spectra show typical uranyl vibration bands in the 770–910 cm^{-1} range, corresponding to symmetrical and asymmetrical UO_2^{2+} uranyl stretching vibrations ν_1 and ν_3 . The obtained vibration values for ν_1 and ν_3 are in good agreement with the mathematical model suggested by Bagnall et al. [31]. The application of Veal et al. [32] empirical equation, relating uranyl bond length $d_{\text{U}=\text{O}}$ to the asymmetric stretching vibration ν_3 for uranyl ions ($d_{\text{U}=\text{O}} = 81.2 (\nu_3)^{-2/3} + 0.895$), leads to the predicted uranyl bond length, in good agreement with the average

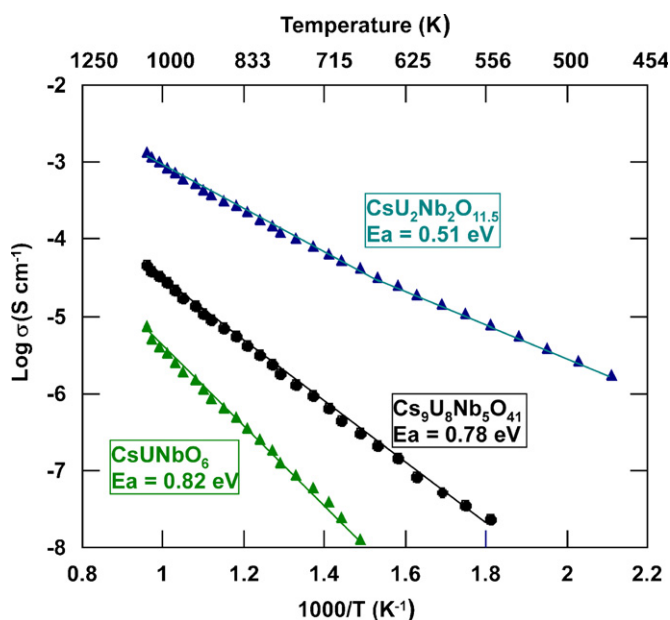


Fig. 6. Arrhenius plots of the electrical conductivity of layered $\text{Cs}_9[(\text{UO}_2)_8\text{O}_4(\text{NbO}_5)(\text{Nb}_2\text{O}_8)_2]$, CsUNbO_6 and tunneled $\text{CsU}_2\text{Nb}_2\text{O}_{11.5}$.

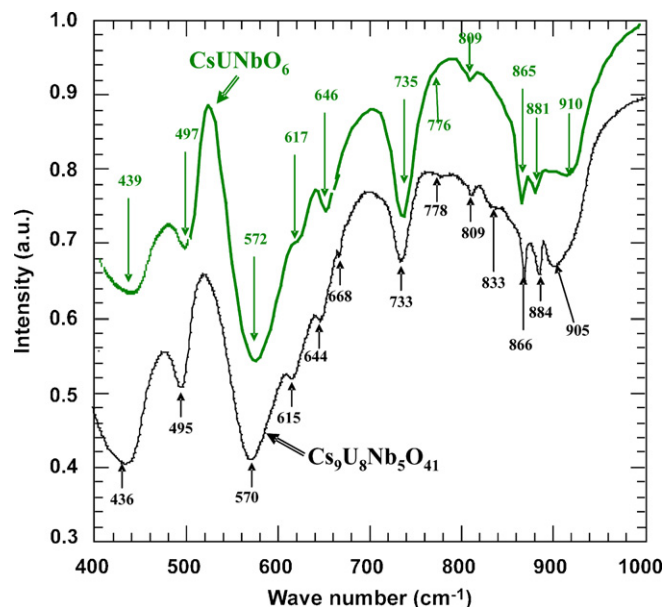


Fig. 7. Infrared spectra of layered compounds $\text{Cs}_9[(\text{UO}_2)_8\text{O}_4(\text{NbO}_5)(\text{Nb}_2\text{O}_8)_2]$ and $\text{Cs}_2[(\text{UO}_2)_2(\text{Nb}_2\text{O}_8)]$.

Table 4
Infrared absorption bands in $\text{Cs}_9[(\text{UO}_2)_8\text{O}_4(\text{NbO}_5)(\text{Nb}_2\text{O}_8)_2]$ and CsUNbO_6

Wave number (cm^{-1})		Vibration mode
$\text{Cs}_9\text{U}_8\text{Nb}_5\text{O}_{41}$	CsUNbO_6	
778–809	776–809	$\nu_1(\text{UO}_2^{2+})$ ss
866–884–905	865–881–910	$\nu_3(\text{UO}_2^{2+})$ as
436–495–570	439–497–572	$\nu(\text{U}-\text{O}_{\text{eq}})$ eq
615–644–668–733	617–646–735	$\text{NbO}_5\text{--Nb}_2\text{O}_8$

ss: symmetric stretching, as: asymmetric stretching, eq: equatorial vibrations.

value obtained from the X-ray structure results. The measured band positions and corresponding vibrations are reported in Table 4. The condensed niobate groups Nb_2O_8 can be considered as the association of Nb_2O_2 double bridges and NbO_3 terminal groups. Thus, the intense bands observed in the range $733\text{--}735\text{ cm}^{-1}$ are probably related to stretching vibrations of NbO_5 and NbO_3 terminal groups and the less intense bands between 610 and 670 cm^{-1} could be assigned to $\nu\text{Nb}_2\text{O}_2$ double bridges.

References

- [1] F. Abraham, S. Obbade, in: S.V. Krivovichev, P.C. Burns, I.G. Tananaev (Eds.), *Structural Chemistry of Inorganic Actinide Compounds*, Elsevier, Amsterdam, 2007, p. 279.
- [2] S. Surblé, S. Obbade, S. Saad, S. Yagoubi, C. Dion, F. Abraham, *J. Solid State Chem.* 179 (2006) 3238.
- [3] M. Gasperin, *Acta Crystallogr. C* 43 (1987) 404.
- [4] F. Abraham, C. Dion, N. Tancret, M. Saadi, *Adv. Mater. Res.* 1–2 (1994) 511.
- [5] M. Saadi, Thesis, Lille, 2001.
- [6] P.B. Barton, *J. Am. Miner.* 43 (1958) 799.
- [7] F. Cesbron, N. Morin, *Bull. Soc. Fr. Minéral. Cristallogr.* 91 (1968) 453.
- [8] F. Cesbron, *Bull. Soc. Fr. Minéral. Cristallogr.* 93 (1970) 242.
- [9] J. Borene, F. Cesbron, *Bull. Soc. Fr. Minéral. Cristallogr.* 93 (1970) 426.
- [10] F. Cesbron, *Bull. Soc. Fr. Minéral. Cristallogr.* 93 (1970) 320.
- [11] J. Borene, F. Cesbron, *Bull. Soc. Fr. Minéral. Cristallogr.* 94 (1971) 8.
- [12] P.G. Dickens, C.P. Stuttard, R.G.J. Ball, A.V. Powell, S. Hull, S. Patat, *J. Mater. Chem.* 2 (2) (1992) 161.
- [13] D.E. Appleman, H.T. Evans, *J. Am. Miner.* 50 (1965) 825.
- [14] H.M. Rietveld, *Acta Crystallogr.* 22 (1967) 151.
- [15] H.M. Rietveld, *Acta Crystallogr.* 25 (1992) 589.
- [16] J. Rodrigez Carvajal, M.T. Fernandez Diaz, J.L. Martinez, *J. Phys.: Condens. Matter* 3 (1991) 3215.
- [17] C. Caglioti, A. Paoletti, E.P. Ricci, *Nucl. Instrum. Methods* 3 (1958) 223.
- [18] SAINT Plus, Version 5.00, Bruker Analytical X-ray Systems, Madison, WI, 1998.
- [19] R.H. Blessing, *Acta Crystallogr. A* 51 (1995) 33.
- [20] J.A. Ibers, W.C. Hamilton (Eds.), *International Tables for X-Ray Crystallography*, vol. IV, Kynoch Press, Birmingham, UK, 1974.
- [21] G.M. Sheldrick, SHELXS-86, Program for Crystal Structure Determination, University of Göttingen, Germany, 1986.
- [22] SHELXTL NT, Program Suite for Solution and Refinement of Crystal Structure, Version 5.1, Bruker Analytical X-rays Systems, Madison, WI, 1998.
- [23] P.C. Burns, R.C. Ewing, F.C. Hawthorne, *Can. Mineral.* 35 (1997) 1551.
- [24] N.E. Brese, M. O'Keeffe, *Acta Crystallogr. B* 47 (1991) 192.
- [25] S. Obbade, C. Dion, E. Bekaert, S. Yagoubi, M. Saad, F. Abraham, *J. Solid State Chem.* 172 (2003) 305.
- [26] S. Yagoubi, Ph.D. Thesis, University of Sciences and Technologies of Lille, 3 December 2004.
- [27] E.V. Alekseev, E.V. Suleimanov, M.O. Marychev, E.V. Chuprunov, G.K. Fukin, *J. Struct. Chem.* 47 (2006) 886.
- [28] S.V. Krivovichev, P.C. Burns, *Can. Mineral.* 41 (2003) 1225.
- [29] P.C. Burns, *Can. Mineral.* 43 (2005) 1839.
- [30] M. Gasperin, *J. Solid State Chem.* 67 (1987) 219.
- [31] K.W. Bagnall, M.W. Wakerley, *J. Inorg. Nucl. Chem.* 37 (1) (1975) 329.
- [32] B.W. Veal, D.J. Lam, W.T. Carnall, H.R. Hestra, *Phys. Rev. B* (1975) 5651.